



HAL
open science

Kinetic data acquisition in high-throughput Fischer-Tropsch experimentation

Paul Hazemann, Dominique Decottignies, Sylvie Maury, Séverine Humbert,
Adrien Berliet, Cécile Daniel, Yves Schuurman

► **To cite this version:**

Paul Hazemann, Dominique Decottignies, Sylvie Maury, Séverine Humbert, Adrien Berliet, et al.. Kinetic data acquisition in high-throughput Fischer-Tropsch experimentation. *Catalysis Science & Technology*, 2020, 10 (21), pp.7331-7343. 10.1039/d0cy00918k . hal-02939257

HAL Id: hal-02939257

<https://hal.science/hal-02939257>

Submitted on 4 Jan 2021

HAL is a multi-disciplinary open access archive for the deposit and dissemination of scientific research documents, whether they are published or not. The documents may come from teaching and research institutions in France or abroad, or from public or private research centers.

L'archive ouverte pluridisciplinaire **HAL**, est destinée au dépôt et à la diffusion de documents scientifiques de niveau recherche, publiés ou non, émanant des établissements d'enseignement et de recherche français ou étrangers, des laboratoires publics ou privés.

Catalysis Science & Technology

Accepted Manuscript

This article can be cited before page numbers have been issued, to do this please use: P. Hazemann, D. Decottignies, S. Maury, S. Humbert, A. Berliet, C. Daniel and Y. Schuurman, *Catal. Sci. Technol.*, 2020, DOI: 10.1039/D0CY00918K.



This is an Accepted Manuscript, which has been through the Royal Society of Chemistry peer review process and has been accepted for publication.

Accepted Manuscripts are published online shortly after acceptance, before technical editing, formatting and proof reading. Using this free service, authors can make their results available to the community, in citable form, before we publish the edited article. We will replace this Accepted Manuscript with the edited and formatted Advance Article as soon as it is available.

You can find more information about Accepted Manuscripts in the [Information for Authors](#).

Please note that technical editing may introduce minor changes to the text and/or graphics, which may alter content. The journal's standard [Terms & Conditions](#) and the [Ethical guidelines](#) still apply. In no event shall the Royal Society of Chemistry be held responsible for any errors or omissions in this Accepted Manuscript or any consequences arising from the use of any information it contains.

ARTICLE

Kinetic data acquisition in high-throughput Fischer-Tropsch experimentation

Paul Hazemann,^{a,b} Dominique Decottignies,^a Sylvie Maury,^a Séverine Humbert,^a Adrien Berliet,^a Cécile Daniel,^b Yves Schuurman^{*,b}

Received 00th January 20xx,
Accepted 00th January 20xx

DOI: 10.1039/x0xx00000x

The emergence of high-throughput experimentation gives new opportunities for accurate and rapid data acquisition for a wide variety of chemical reactions in different fields of application such as hydrocracking, isomerization and syngas conversion. Fischer-Tropsch synthesis is a challenging reaction to carry out due to its exothermicity, its wide range of products including heavy waxes, catalysts sensitivity to deactivation and the large number of parameters influencing the kinetics. Despite the accuracy gain brought by the most recent high-throughput technologies, numerous parameters need to be controlled for accurate data acquisition and correct comparison of catalysts performances. The present study shows that the high-throughput test strategy plays a major role and can affect significantly the accuracy and coherence of the generated data. For instance, when catalysts performances are measured for kinetic purposes, a common used method to vary the contact time (W_{cat}/F_{CO}) is by loading the reactors with different amounts of catalyst. However, this method is not suited for catalysts that are difficult to reduce, since it has been shown that hydrogen space velocity during catalyst reduction has an influence on the degree of the reduction of the catalyst. Still this method might be preferred over the method of varying the syngas flowrate for a constant catalyst weight. The latter is time consuming and introduces deviations because of catalysts deactivation with time on stream. This issue becomes particularly important when liquid composition analysis is required, since even with miniaturized high-throughput setup we observed significant transitory periods on the liquid composition, due to wax accumulation in post-reactor volumes or to catalyst evolution such as deactivation or surface reconstruction. Deactivation could, however, be limited by operating at low conversion levels or by running successive short tests.

1. Introduction

Fischer-Tropsch synthesis (FTS) is a promising route for clean fuels¹ and sustainable chemicals production via the xTL process, in which biomass (BtL), coal (CtL) or natural gas (GtL) can be used as raw materials. Efficient Fischer-Tropsch catalysts are crucial to make the process economically viable and competitive with conventional petroleum-based routes. However, the evaluation of new catalyst performances can be time consuming and costly². To overcome this issue, two strategies can be employed: the first one is the use of fast characterization techniques, for which the analysed properties are directly linked to catalysts performances. For instance, Boldrin et al.³ proposed an efficient way to accelerate Fischer-Tropsch catalysts screening using High-Throughput TGA and XRD. The second one, chosen by more and more research groups^{4–9}, is the use of parallelized and miniaturized reactor

setups, more commonly known as high-throughput experimentation (HTE). Van der Waal et al.¹⁰ demonstrated the potential of such a technology for FTS by characterizing the coherence of the data generated with 64 fixed-bed reactors operated in parallel. A high repeatability of the catalysts performances between reactors was obtained (95%), and the selectivity measured by on-line gas chromatography was in good agreement with the off-line liquid phase analysis. A strong repeatability of reactor to reactor data was also obtained by Cao et al.¹¹ on a multi-channel microtubular reactor setup, with a similar standard deviation. Because of its high accuracy, the HTE technology is recognized as a powerful tool to acquire a large amount of data in a short period of time, making it suitable for catalysts screening, kinetic modelling and mechanistic understanding^{2,10,12,13}. Several issues are, however, important to consider when operating such experimental setups, in order not to compare incoherent data and make biased conclusions. For instance, Van der Waal¹⁰ and Cao¹¹ both underlined the necessity to use sufficiently small reactor diameter to avoid heat and mass transfer limitations ($< 2 \text{ mm}^{10}$), which are particularly important when data is acquired for kinetic studies. Small reactor diameter have also been recommended by Chambrey et al.¹⁴ to better control temperature during the

^a IFP Energies nouvelles, Rond-Point de l'Echangeur de Solaize-BP3, Solaize 69360, France

^b Univ Lyon, Université Claude Bernard Lyon 1, CNRS, IRCELYON, F-69626, Villeurbanne, France

* yves.schuurman@ircelyon.univ-lyon1.fr

reactor start up. Because of the high exothermicity^{15,16} of the Fischer-Tropsch reaction ($\Delta H_r = -167 \text{ kJ mol}^{-1}$ for CH_2 monomer formation¹⁵), the first exposition of the catalyst to syngas may indeed lead to an uncontrolled temperature increase and provoke undesired deactivation. This is a recurring issue in conventional fixed bed reactors, for which radial heat transfer is low. It can be avoided in HTE, by the use of milli-fixed bed reactors.

The accuracy of the data obtained by HTE might also depend on other factors, where the test methodology plays a major role. Xiao et al.¹⁷ reported several phenomena that could impact significantly the Fischer-Tropsch product analysis. Particular attention should be paid to heavy product accumulation, which can induce severe deviations from the Anderson-Schulz-Flory distribution if the reactor is not operating in steady state. A certain period of time is required for the dense products to fill the downstream dead volumes and thus to be collected, whereas the light products (typically in gaseous state) rapidly reach the collection system because of their higher molar volume. Deactivation is also an important parameter to consider, in particular if performance evaluation is carried out for long Time On Stream (TOS). Chambrey et al.¹⁴ showed that even if catalysts are less sensitive to deactivation in milli-fixed bed reactors, the activity loss can reach $1\% \cdot \text{day}^{-1}$, which is significant when tests are carried out for hundreds of hours. To avoid this issue, Morra et al.¹⁸ used a HTE setup which can feed one reactor with a fixed composition and the other ones with a different composition. This configuration allows the acquisition of kinetic data under different conditions on a selected reactor, while the others are running under non-deactivating conditions (inert feed). The data acquisition is then performed successively reactor after reactor, and the overall data set is thus representative of the initial catalyst state for every reactor. However, to reduce the costs and improve accuracy, most recent HTE setups embed specific systems such as mutualized feed distributions¹⁰, pressure regulators^{10,11,13} or heating blocks^{10,11,13} making it impossible to choose different operating conditions from one reactor to the other, such as flowrate, flow composition and pressure. To face this problem, alternative strategies have been used, for instance contact time variations by loading^{2,4,12,13,18} different amount of the same catalyst in different reactors, which is particularly interesting for kinetic studies. This method may, however, introduce some differences between the different reactors since as a consequence, the catalysts are also activated at different hydrogen space velocities from one reactor to another, and their performances can be affected. A way to ensure a uniform degree of reduction between each reactor is the use of reduction promoters, but this method might not be suited for kinetic studies because of the promoters potential involvement in Fischer-Tropsch reactions¹⁹.

The present study discusses the suitability of HTE for kinetic studies, dealing with several issues frequently encountered in Fischer-Tropsch synthesis: catalysts activation and deactivation, mass transfer limitations, and wax accumulation. The effect of hydrogen space velocity on non-promoted catalysts activation

will first be studied, and the accuracy of the data obtained in HTE will then be evaluated on a 16-reactor setup. Effects of operating conditions will be studied and compared to the data from literature. A focus on contact time variation methods will be carried out in particular to assess their suitability for kinetic studies. Deactivation and steady state product analysis will finally be discussed.

2. Experimental

2.1 Catalysts synthesis

Two 15 wt.% Co catalysts were prepared by incipient wetness impregnation, using commercial *Siralox5* (silica alumina from Sasol) as a support. An aqueous $\text{Co}(\text{NO}_3)_2 \cdot 6\text{H}_2\text{O}$ solution was employed as a source of cobalt, and two successive impregnations were performed to reach the desired cobalt loading. The impregnated catalysts were then dried and calcined with two different protocols in order to obtain two different cobalt particle sizes. The first catalyst (referred as Co-12) was dried in a static oven at 85°C for 12 hours before being calcined in air ($2 \text{ NL} \cdot \text{h}^{-1} \cdot \text{g}^{-1}$) with a fixed bed reactor for 2 hours, at 400°C using a heating ramp of $2.5^\circ\text{C} \cdot \text{min}^{-1}$. The other catalyst (Co-18) was pre-dried at 85°C for 30 minutes in a static oven, before being transferred into a fluidized bed reactor where the main drying step occurred. This last step consisted of exposing the catalyst to an air flow with a gas velocity of $0.8 \text{ NL} \cdot \text{h}^{-1} \cdot \text{g}^{-1}$ of support, at 100°C for 2 hours. The heating ramp from room temperature to 100°C was $1.5^\circ\text{C} \cdot \text{min}^{-1}$. The subsequent calcination was conducted directly in the same reactor, at 400°C for 2 h using an air flow of equivalent gas velocity. The heating ramp from 100 to 400°C was $5^\circ\text{C} \cdot \text{min}^{-1}$.

2.2 Catalysts characterization

The specific surface area and pore volume of the cobalt oxide catalysts were measured by nitrogen physisorption using an Asap® 2420 instrument from Micromeritics®. The specific surface area was estimated with the BET method and the pore volume was considered to be equivalent to the nitrogen volume adsorbed at maximum pressure.

Cobalt oxide (Co_3O_4) average particle sizes were determined by X-Ray Diffraction (XRD). Diffractograms were registered on a PANalytical X'Pert Pro® apparatus equipped with a copper source ($\lambda_{\text{CuK}\alpha 1} = 1.5406 \text{ \AA}$). The Co_3O_4 average particle size was calculated using the Scherrer method on oxide catalysts and the metallic cobalt particle size was estimated to be equal to 0.80 the size of the Co_3O_4 particle (molar volume ratio of Co over Co_3O_4). The metallic cobalt particle size distribution was also estimated by Transmission Electron Microscopy (TEM). TEM images of reduced and passivated catalysts were taken in dark field mode for a better contrast, with a JEM 2100F microscope. Particle size distributions were based on the measurement of more than 200 particles, and the average particle size in volume was estimated by fitting the particle size distribution with a log normal law. The catalyst reduction before TEM analysis was performed in a 5 mm ID reactor at 400°C for 16h, using a

hydrogen gas velocity of $2 \text{ NL h}^{-1} \text{ g}^{-1}$ and a heating ramp of 2°C min^{-1} . The samples were then passivated at room temperature with a mixture of 1% O_2/N_2 for 3h before unloading the catalysts.

To quantify the catalysts active sites and to corroborate the particle size at a given degree of reduction with XRD and TEM results, static H_2 -chemisorption was performed using a BELSORP-max apparatus over catalysts that were reduced at 350°C under pure hydrogen for 2h. The degree of reduction (DOR) of the samples was controlled after the analysis by Temperature Programmed Reduction (TPR), using the procedure described below. Knowing the catalysts DOR, the average particle size was calculated from the number of surface cobalt atoms considering a spherical particle shape. Hydrogen was considered to adsorb dissociatively on metallic cobalt²⁰, thus the number of active sites corresponds to twice the number of adsorbed H_2 molecules.

TPR analysis was performed with an AutoChem II 2920 V4.03 apparatus from Micromeritics®. 0.5 g of catalyst was exposed to 58 NmL min^{-1} of 5% H_2/Ar while heating from room temperature to 1000°C at 5°C min^{-1} . The technique was either used to qualitatively estimate the catalysts reducibility, but also performed to quantify the degree of reduction of reduced catalysts. In practice, the CoO area of the reduced passivated catalyst profile was subtracted from the CoO area of the catalyst precursor obtained after the calcination profile to determine the fraction of unreduced cobalt.

Magnetization measurements were used to determine the fraction of metallic cobalt of the catalyst. Metallic cobalt exhibits a high magnetic susceptibility compared to its oxide or carbide phases^{21–25}. Knowing the theoretical magnetization of a sample corresponding to hundred percent metallic fraction, and by neglecting the susceptibility of the non-metallic cobalt phases the actual DOR is given by the relation:

$$\text{DOR} = \frac{M_s}{\sigma \cdot m} \quad (\text{Eq. 1})$$

M_s being the saturation magnetization, σ the magnetic susceptibility of metallic cobalt, and m the cobalt mass of the sample. The saturation magnetization was estimated at a magnetic field of 2T.

2.3 High-throughput experiments

Table 1: Evaluation of different criteria to assess the intrinsic kinetic conditions. For the calculations, the standard reaction conditions were used (see main text) and $r_{\text{CO,max}} = 0.012 \text{ mol}\cdot\text{kg}_{\text{cat}}^{-1}\cdot\text{s}^{-1}$. h : catalyst bed length, d_p : catalyst particle diameter, D_R : reactor diameter.

Physical phenomenon	Criteria
plug flow (axial)	$h/d_p = 1100 > 7$
plug flow (radial)	$D_R/d_p = 17 > 10$
external mass transfer (Carberry number)	$1 \cdot 10^{-5} < 0.05$
internal mass transfer (Wheeler-Weisz)	$1 \cdot 10^{-3} < 0.08$
external heat transfer (film)	$0.01 \text{ K} < 1.2 \text{ K}$
external heat transfer (radial)	$0.4 \text{ K} < 1.2 \text{ K}$
internal heat transfer	$0.001 \text{ K} < 1.2 \text{ K}$

The HTE setup used is a Flowrence® unit developed by Avantium (Figure 1). Sixteen down-flow fixed bed reactors (2 mm ID) run in parallel with a mutual gas feed, equally distributed through the reactors by a patented passive micro-chip. The relative standard deviation of the flowrate measured on the different reactors without any catalyst is less than 2%. Pressure is regulated for each reactor independently around a common set point, and is based on the values measured at the entrance of the reactors. Four independent heating blocks are used to control the temperature of 4 reactors each. Temperatures are measured at three heights of the heating blocks to ensure the temperature homogeneity along the catalytic beds. The reactor isothermal zone ($\pm 0.7^\circ\text{C}$ at 250°C) measures 20 cm starting from 8 cm of the bottom. The catalyst bed (100 mg – 500 mg) is placed within this isothermal zone on top of a 10 cm layer of ceramic powder (Microblast® B-120). A second layer of ceramic powder is placed on top of the catalyst layer to reach a total bed length of 40 cm. The last 16 cm of the reactor are filled using a 1 mm glass sock, to minimize dead volumes and improve gas mixing. Effluents are collected downstream and heavy products are separated from the light ones by a cold trap at 80°C . Light products up to C_{10} hydrocarbons are analysed on-line by gas chromatography and heavy products off-line by simulated distillation analysis. Based on thermodynamic calculations using PRO/II software (SRK model), C_{10} -products are recovered at 95% in the gaseous phase and C_{17+} at 95% in the liquid phase. Helium is used as an internal standard for gas flow calculation and is analysed by a thermal conductivity detector (TCD), along with N_2 , CO , and H_2 , which are separated through a molecular sieve column. The lightest hydrocarbons cut ($\text{C}_1\text{--}\text{C}_8$) is separated from the heavy

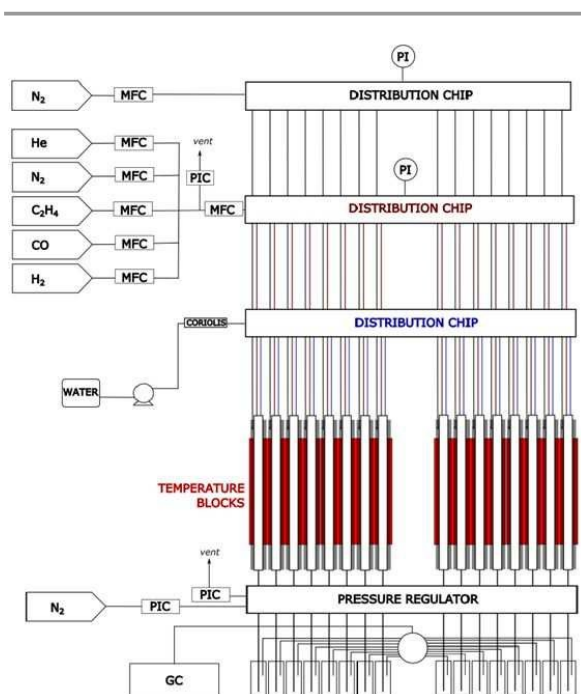


Figure 1: Schematic of the HTE 16-reactor Fischer-Tropsch unit

hydrocarbons one (C₉–C₁₄) by a first HP-INNOWax column. Light hydrocarbons are then separated through a GS-GasPro column, and heavy ones through a second HP-INNOWax column. Both hydrocarbons cuts are finally analysed with a flame ionisation detector (FID). CO₂ is converted into methane over a Ni catalyst before being analysed on the heavy products column. Water is not quantified, and since some heavy products are not fully condensed at 80°C, element balance cannot be calculated.

The total outlet flowrate Q_{out} is calculated according to the formula

$$Q_{out} = \frac{Q_{He, in}}{V_{He, out}} \quad (\text{Eq. 2})$$

$Q_{He, in}$ is the inlet flowrate of helium, and $V_{He, out}$ is the measured outlet volume fraction of helium. Specific flowrates $Q_{i, out}$ of compounds i are then calculated as

$$Q_{i, out} = Q_{out} \cdot V_{i, out} \quad (\text{Eq. 3})$$

$V_{i, out}$ is the concentration of compound i at the outlet. CO conversion, CH₄, C₂, C₃, C₄ and C₅₊ selectivity are obtained by the following relations:

$$X_{CO} = \frac{Q_{CO, in} - Q_{CO, out}}{Q_{CO, in}} \quad (\text{Eq. 4})$$

$$S_{CH_4} = \frac{Q_{CH_4, out}}{Q_{CO, in} - Q_{CO, out}} \quad (\text{Eq. 5})$$

$$S_{C_2} = \frac{2 \cdot Q_{C_2, out}}{Q_{CO, in} - Q_{CO, out}} \quad (\text{Eq. 6})$$

$$S_{C_3} = \frac{3 \cdot Q_{C_3, out}}{Q_{CO, in} - Q_{CO, out}} \quad (\text{Eq. 7})$$

$$S_{C_4} = \frac{4 \cdot Q_{C_4, out}}{Q_{CO, in} - Q_{CO, out}} \quad (\text{Eq. 8})$$

$$S_{C_{5+}} = 1 - (S_{CH_4} + S_{C_2} + S_{C_3} + S_{C_4}) \quad (\text{Eq. 9})$$

The catalysts activity was followed through the CO consumption rate divided by the catalyst mass, noted r_{CO} (in $\mu\text{mol} \cdot \text{s}^{-1} \cdot \text{g}^{-1}$) and defined as:

$$r_{CO} = \frac{X_{CO} \cdot Q_{CO, in}}{V_{m, CO} \cdot m_{catalyst}} \quad (\text{Eq. 10})$$

with $V_{m, CO}$ the CO molar volume under standard conditions of temperature and pressure and $Q_{CO, in}$ the CO inlet flowrate (NL s⁻¹).

During the tests, one of the 16 reactors is kept empty to verify that both the feed distribution and analysis of the products are correct. The measured CO conversion in this reactor should be 0%, any deviation would indicate a default of either the analytical system or of the feed section.

For each test, catalysts are reduced in-situ under 0.45 NL h⁻¹ of pure hydrogen at 400°C for 16 h, with a heating ramp of 2°C min⁻¹ at atmospheric pressure. The temperature is then decrease to 180°C under hydrogen and the pressure is progressively raised to 20 barg. Syngas is finally injected and the temperature increased to 220°C with a ramp of 1°C min⁻¹. The syngas GHSV used in the tests were comprised between 2 and 13 NL h⁻¹ g⁻¹, and the H₂/CO molar ratios between 1.85 and 2.4.

Heat and mass transfer are considered not to be limiting factors according to the calculations presented in Table 1, for which the details can be found elsewhere²⁶. All criteria to assume ideal intrinsic kinetic conditions are fulfilled.

2.4 Slurry reactor tests

Before Fischer-Tropsch slurry experiments, the catalyst activation was performed in a fixed bed reactor using the same protocol as for HTE, but with a H₂ flowrate of 2 NL h⁻¹ g⁻¹. The catalyst was then unloaded under inert gas and coated with n-C₂₂ solvent to prevent re-oxidation. The n-C₂₂ catalyst sample was let to solidify before being transferred into the slurry reactor previously filled with n-C₂₂. Then slurry experiments were carried out in a 50 cm³ CSTR at 220°C, 20 barg, molar ratio H₂/CO = 2.12. A known mass of 3 to 4 g of reduced embedded catalyst was loaded in the reactor, and the syngas space velocity was adjusted at the beginning of the test to reach 45% CO conversion. The conversion was then followed with time on stream like the HTE fixed bed experiments in which no gas velocity change is applied. Gas phase analysis was carried out on-line using a Molecular Sieve column with a TCD for permanent gases, and a PONA column with a FID for light hydrocarbons. The relative standard deviation of the GC analysis was estimated to 3%.

2.5 Wax composition analysis

The liquid product fraction (typically C₁₇₊ hydrocarbons) was analysed off-line by simulated distillation. The hydrocarbon mix (typically 0.1 g) was dissolved in CS₂ before being separated through a MXT[®]-1 column, after which hydrocarbons were quantified by a FID. The chain growth probability α was calculated based on the C₁₇₋₄₂ hydrocarbons distribution, by fitting the Anderson-Schulz Flory (ASF) equation²⁷.

3. Results

3.1 Catalysts properties

Oxide catalysts main textural properties are presented in Table 2. No major difference is observed between the two catalysts, which both exhibit slightly lower surface area and pore volume than the support (171 m² g⁻¹, 0.52 mL g⁻¹), probably due to pore blockage by cobalt oxide particles²⁸.

The average particle size of the two catalysts given by the different techniques mentioned in section 2.3 are also listed in Table 2. For each method, the Co-18 catalyst shows a larger particle size than the Co-12 one. For instance, a value of 18±2 nm is obtained by XRD for the Co-18 oxide catalyst while a value of only 12±1 nm is found for the Co-12 one. The average particle

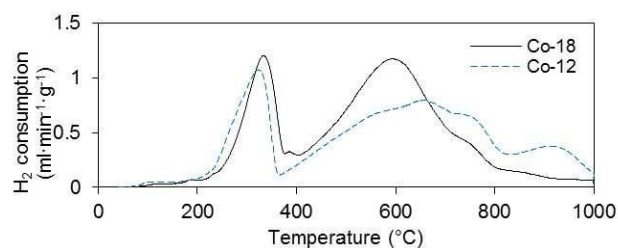


Figure 2: Temperature Programmed reduction profiles of the two catalysts

size of reduced catalysts can be deduced from these values, considering the molar volumes of Co^0 and Co_3O_4 ($v_{\text{Co}}/v_{\text{Co}_3\text{O}_4} = 0.80$). The average particles sizes of the reduced catalysts are estimated to be 14 nm and 10 nm for the Co-18 and Co-12, respectively. Particle sizes calculated from TEM images corroborated rather well these calculations since they were found as 11 ± 1 nm for the Co-12 catalyst and 12 ± 1 nm for the Co-18 one. *In-situ* magnetisation measurements showed that passivation reduces the DOR of both catalysts by 25%, which corresponds to a passivation layer of 0.6 nm considering a spherical particle shape. The reduced catalyst particle sizes are therefore estimated to 12 nm and 13 nm for Co-12 and Co-18, respectively. Although the difference between the two is less by TEM method than by XRD, a larger particle size is found for the Co-18 catalyst. The same observation is made for the H_2 chemisorption measurements, with particle sizes of 15 nm and 17 nm for the Co-18 and Co-12, respectively. Despite an overestimation, these values are in good agreement with the XRD results. Both TEM and H_2 chemisorption indicate less of a difference in the average particle size between the two catalysts after reduction. This could be due either to sintering of small particles during reduction, or to preferential reduction of big particles.

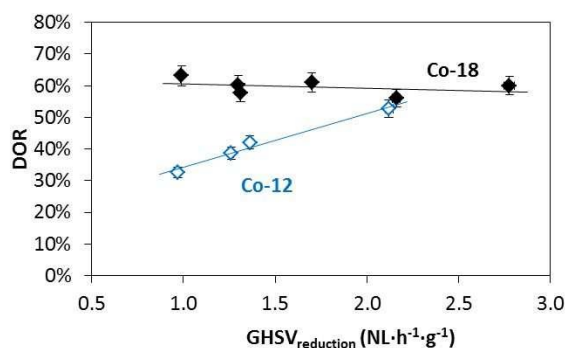
TPR profiles of the two catalysts are presented in Figure 2, which clearly show the particle size effect on the catalyst reducibility. The first peak of H_2 consumption (300°C) corresponds to the reduction of Co_3O_4 into $\text{CoO}^{29,30}$, whereas the second one correspond to the reduction of CoO into Co^0 . While no significant difference can be observed for the first peak, the second peak is slightly shifted to higher temperatures for the Co-12 catalyst. This might be due to the high metal-support interactions of small particles that decrease the catalyst's reducibility^{31,32}.

3.2 Effect of hydrogen space velocity on catalysts activation

Table 2: Catalysts textural properties and particles size

	S_{BET} (m^2/g)	V_p (ml/g)	$d_{\text{Co}_3\text{O}_4/\text{XRD}}$ (nm)	$d_{\text{Co}/\text{XRD}}$ (nm)	d_{TEM} (nm)	$d_{\text{TEM corr.}}$ (nm)*	N_{Schem} (mmol/g)**	d_{chem} (nm)
Co-12	139 ± 7	0.37 ± 0.01	12 ± 1	10 ± 1	11 ± 1	12 ± 1	0.10 (62)	15
Co-18	135 ± 7	0.36 ± 0.01	18 ± 2	14 ± 1	12 ± 1	13 ± 1	0.11 (74)	17

*Corrected considering the passivation layer

**Number of active sites estimated by H_2 chemisorption analysis, with in parenthesis the percentage of reduction of the samples (%)Figure 3: Effect of H_2 gas space velocity on catalysts reduction performed in milli-fixed bed reactors

The conversion in a plug flow fixed bed reactor depends on the ratio $W_{\text{cat}}/F_{\text{CO}}$, which is directly related to the mean residence or contact time. The generation of accurate data at different ratios of $W_{\text{cat}}/F_{\text{CO}}$ is therefore essential in kinetic studies. To vary the contact time, one can either vary the mass of catalyst (W_{cat}) or the inlet flow rate (F_{CO}). To take full advantage of the parallelization in HTE, it is best to adapt the catalyst mass in the different reactors^{2,4,12,13,18} and operate all reactors at the same flow rate. This strategy, however, implies that different hydrogen space velocities are applied to all catalyst samples during the *in-situ* catalyst reduction treatment. This parameter has a great influence on the degree of reduction of cobalt and nickel catalysts^{33,34}. Water is the main product of cobalt oxide reduction, and a change in its dilution level may modify the final extent of reduction³⁵ because of a kinetic inhibition³⁶. The effect of the hydrogen space velocity on the catalyst reduction was studied by magnetisation measurements of samples reduced in the HTE setup. The hydrogen space velocity used for reduction was varied from 1.0 to 2.2 $\text{NL h}^{-1} \text{g}^{-1}$, by varying the amount of catalyst from 100 mg to 460 mg (hydrogen flowrate of $0.45 \text{ NL}\cdot\text{h}^{-1}$). Figure 3 shows the two catalyst's DOR's as a function of the GHSV (*Gas Hourly Space Velocity*) used for reduction, performed at 400°C for 16 h in the HTE setup. The DOR's were calculated based on magnetization measurement. After reduction in the HTE unit, the samples were unloaded under inert atmosphere ($<0.5 \text{ ppm O}_2$, $<0.5 \text{ ppm H}_2\text{O}$), to prevent any re-oxidation by air exposure. Two different trends were observed. The less reducible one, Co-12, exhibits a clear dependency of its DOR on the GHSV, with higher DOR's at high hydrogen gas velocity. On the contrary, the Co-18 catalyst is not sensitive to the gas velocity used for reduction, at least for a GHSV range between 1 and 3 $\text{NL h}^{-1} \text{g}^{-1}$. This phenomenon complicates the measurement of kinetics in HTE over catalysts that are difficult to reduce. This may be one of the reasons why

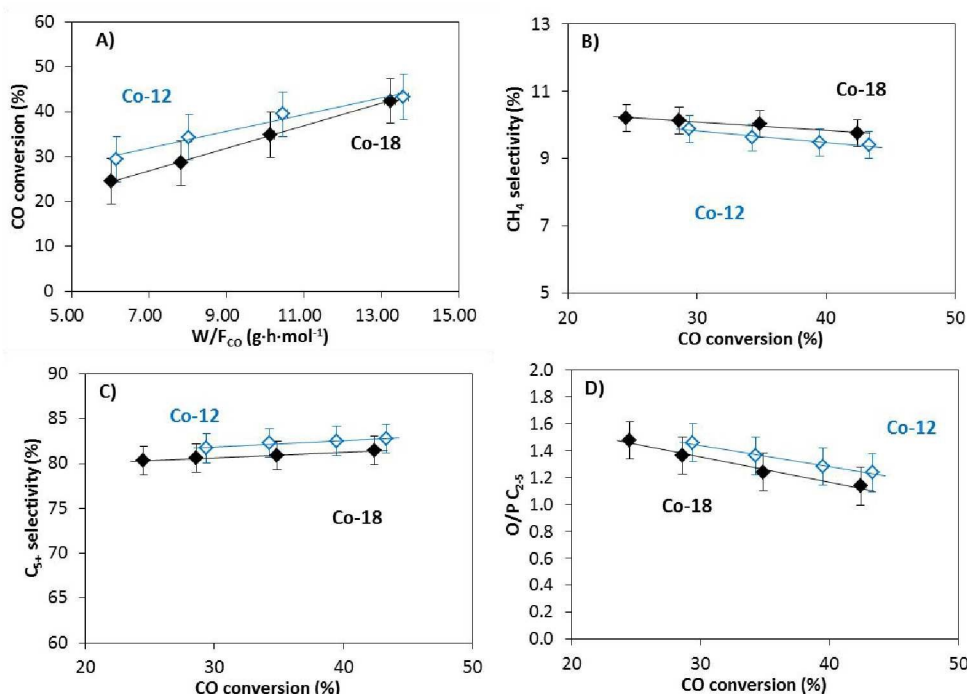


Figure 4: Catalysts performances under standard Fischer-Tropsch conditions (TOS 24h, 20 barg, 220°C, H₂/CO = 2.12, Q_{syn gas} = 2.38 NL·h⁻¹). Data is averaged based on 6 successive tests. Error bars represent the reactor-to-reactor reproducibility for a selected test.

numerous research groups prefer to use reduction promoters such as noble metal to overcome this difficulty in most of their studies.

3.3 Catalysts performances and repeatability

Catalyst performances and HTE measurement repeatability were estimated through six successive tests, performed under conventional Fischer-Tropsch conditions (220°C, 20 barg, molar ratio H₂/CO = 2.12). In each test, the same loading plan was used and four different amounts of the 2 catalysts were loaded in 8 different reactors (Table 3), to measure performances at different CO contact times comprised between 6 and 14 g·h·mol⁻¹. Note that data acquired during these tests were therefore obtained with different degree of reduction (GHSV used for reduction from 1.0 to 2.2 NL h⁻¹ g⁻¹). The amount of the Co-12 catalyst was adjusted based on those of the Co-18 catalyst to reach similar conversion levels for the two catalysts. Since the number of active sites measured by chemisorption was rather similar for both catalysts, their amounts are very

close. Table 3 summarizes the catalyst performances averaged over the six runs, for each reactor. Performances are measured after 24 h of TOS. In line with chemisorption analysis, the two catalysts exhibit similar activities and selectivities. This is in accordance with the observations of Bezemer et al.³⁷ who found no significant impact of particle size on both activity and selectivity above 8 nm. The effect of residence time (*i.e.* CO conversion) on catalysts selectivity is also quite similar for both catalysts (Figure 4) and again consistent with the literature^{38–41}. A slight increase of the C₅₊ and CO₂ selectivity is observed with the increase of the CO conversion, while the CH₄ and olefin selectivity decreases. Todic et al.³⁹ discussed the origin of these behaviours and explained that the C₅₊ and CH₄ selectivity evolution at high conversions were mainly due to water effects^{42–44}. CO₂ production via the water-gas shift reaction increases at high conversion because of the high partial pressure of water, and the olefin selectivity decline is associated with the increased residence time used to reach high conversion, facilitating their re-adsorption. Contradictory

Table 3: Catalysts performances at TOS 24h, 220°C, 20 barg, H₂/CO = 2.12, Q_{syn gas} = 2.38 NL·h⁻¹. Relative standard deviation (RSD) are based on 6 successive tests.

n°	Catalyst mass (mg)		X _{CO} (%)		S _{CH4} (%)		S _{C5+} (%)		S _{CO2} (%)		O/P C _{2-C5}		
	Average	RSD	Average	RSD	Average	RSD	Average	RSD	Average	RSD	Average	RSD	
Co-18	1	205	1.2%	24.5	3.5%	10.2	6.0%	80.3	1.9%	0.20	7.9%	1.47	2.7%
	2	267	0.7%	28.6	4.2%	10.1	4.2%	80.6	1.4%	0.20	5.7%	1.36	1.9%
	3	345	0.9%	34.9	2.6%	10.0	3.0%	80.9	1.1%	0.20	3.3%	1.24	3.5%
	4	449	0.5%	42.4	2.6%	9.7	3.3%	81.5	1.1%	0.21	3.1%	1.14	3.5%
Co-12	5	211	0.4%	29.4	8.3%	9.9	4.2%	81.7	1.1%	0.18	4.1%	1.46	4.1%
	6	274	0.5%	34.3	8.7%	9.6	3.2%	82.3	0.9%	0.18	5.2%	1.36	4.2%
	7	355	0.7%	39.5	8.7%	9.5	2.6%	82.5	0.8%	0.19	2.9%	1.28	3.4%
	8	458	0.4%	43.3	9.1%	9.4	2.7%	82.7	0.8%	0.20	3.0%	1.20	2.0%

trends have sometimes been reported at high conversion^{45,46}, but Ma et al.⁴⁷ explained this by the rapid deactivation of the catalyst that occurs at high conversion, changing the degree of oxidation and therefore the selectivity. It can also be due to the high partial pressure of water produced at high conversion levels, which promote the water-gas-shift reaction and thus modify the H₂/CO ratio.

The reactor-to-reactor repeatability of catalyst performances is quite similar to the one reported by van der Waal et al.¹⁰ on a 64-reactor setup, with a RSD value of maximum 5% on activity. However, the inter-test repeatability of catalysts performances is a bit lower than this reactor-to-reactor repeatability, with a RSD value that reaches 10% on CO conversion (Table 3). This difference may be due to the error added by the systematic, but necessary recalibration of the analytical system performed at the beginning of each test. A lower accuracy of catalysts performances measurements should therefore be considered if data is acquired through several tests. Besides, the CO conversion RSD values are higher for the Co-12 catalyst than the Co-18 one. This might be due to the lower reducibility of Co-12, which makes its performance more sensitive to the reduction GHSV. Finally, no effect of the catalyst amount on the error margin is observed within the range operated.

3.4 Steady state

When catalysts are exposed to syngas at the early stage of reaction they generally undergo a transitory period. During this phase their performances are evolving and may not be representative of those at longer TOS. Steady state has to be reached if data is acquired during extended periods. Two phenomena may be at the origin of this behaviour: catalyst surface reconstruction⁴⁸, and hydrodynamic changes due to accumulation of waxes¹⁷ in the catalyst bed and porosity. The period duration can be estimated by monitoring the catalyst activity or selectivity either by gas phase or liquid phase analysis. However, considering the low flowrate of the liquid product fraction, the transitory period for the determination of this fraction composition may be longer than for the gas phase¹⁷. The 24 h catalytic tests showed that the initial transitory period of surface reconstruction and pore filling is fast enough not to be detected by the gas phase analysis. After the first gas analysis registered at TOS 1h the CO conversion decreased continuously, which is likely related to catalyst deactivation. To monitor the evolution of the composition of the liquid fraction, a dedicated HTE test was carried out during an extended period while collecting samples every 12 h. Two different operating conditions were tested successively in order to measure also the transitory period after a change of reaction conditions (lower H₂/CO value). Figure 5 shows the evolution of the liquid productivity and chain growth probability with TOS for the Co-18 catalyst (338 mg). During the first 24 h the liquid fraction productivity increased due to its accumulation inside the downstream dead volume, which represents 0.46 mL. Considering a liquid density of 0.95 g mL⁻¹ and a liquid productivity of 100 mg h⁻¹ g⁻¹, 12h are required to fill this

downstream section with waxes, which corroborates well with our measurements. Chain growth probability is also increasing during this initial period, but in an extent that remains within the error margin. Still, this behaviour could be due to a more severe hold up of heavy hydrocarbons^{48,49}. During the first stage of reaction where the catalyst pores are filled, the heavy hydrocarbons are accumulating in a greater extent than lighter ones⁴⁹ leading to product segregation and thus an underestimation of the chain growth probability. The surface reconstruction could also be at the origin of this behaviour. Several authors have reported an increase in the heavy compound selectivity in the gas phase^{17,48}. A third explanation of this behaviour could be the sintering of the smallest particles. This phenomenon is known to occur mainly at the beginning of the reaction⁵⁰, and it has been shown that larger particles (over 8 nm) exhibit a higher selectivity towards heavy compounds than small ones³⁷. Starting from 36 h of TOS, both productivity and chain growth probability reach a stable value.

After the change of the reaction conditions, an increase of the alpha value is measured, whereas the liquid productivity remains almost constant. No particular transitory period is observed during this condition change for the liquid composition, the alpha value being relatively constant after the first measurement.

Whereas no significant delay is required for the gas phase analysis to obtain representative catalysts performances at a given condition, a transitory period should be respected for accurate liquid phase analysis especially during the reactor start-up. This period should at least exceed the time necessary to fill the dead volume after the reactor, which is correlated to the catalyst liquid productivity. Despite very slight variations of the liquid composition observed during the first 36 h of reaction, it is preferable to perform liquid collection after this period to ensure a representative composition. This constraint dramatically extends the test duration if liquid phase analysis is required and operating conditions are tested successively. In this case, catalyst deactivation becomes an important parameter to consider for coherent data acquisition.

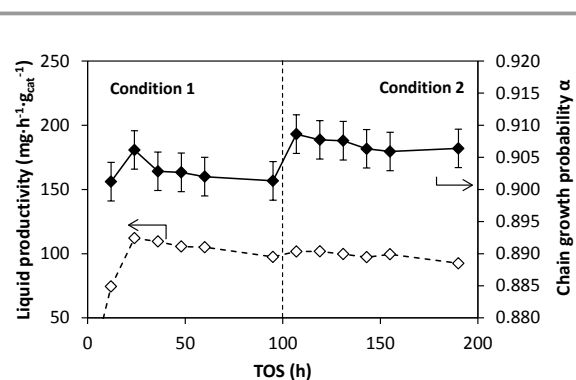


Figure 5: Liquid fraction productivity and composition evolution, at initial reaction stage and during a condition change (CO conversion range: 30–40%). Condition 1 : 220°C, 20 barg, H₂/CO = 2.12, 3.4 NL·h⁻¹·g⁻¹. Condition 2 after 100h TOS : 220°C, 20 barg, H₂/CO = 1.85, 3.2 NL·h⁻¹·g⁻¹.

Table 4 : Catalysts performances in milli-fixed bed reactor compared to slurry bubble reactor at 220°C, 20 barg, H₂/CO = 2.12. Catalysts tested in HTE were reduced under H₂ flow between 1.3 and 1.7 NL·h⁻¹·g⁻¹.

		GHSV (NL·h ⁻¹ ·g ⁻¹)	r _{CO} (μmol·g ⁻¹ ·s ⁻¹)	X _{CO} (%)	S _{CH4} (%)	S _{C5+} (%)	S _{CO2} (%)	O/P C ₂ -C ₅
Co-18	HTE	5.1	9.3	46	10.4	80.0	0.28	1.18
	Slurry	5.3	7.8	37	10.2	76.7	0.35	0.96
Co-12	HTE	3.0	8.0	67	9.6	81.8	0.30	1.01
					12.2	76.8	0.48	0.67

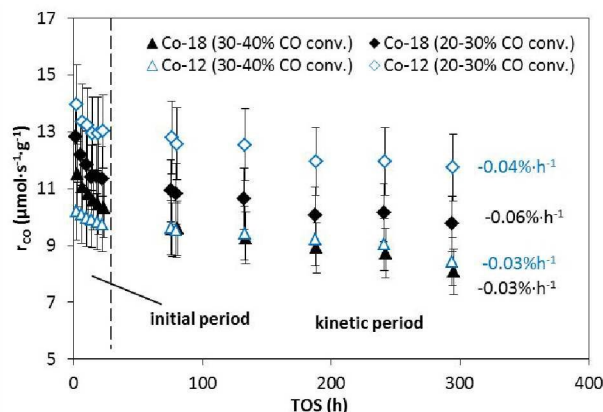


Figure 6 : Deactivation behaviour of the two catalysts at different conversion levels (220°C, 20 barg, H₂/CO = 2.12). Syngas GHSV of 7 and 12 NL·h⁻¹·g⁻¹ were used to reach 30-40% and 20-30% CO conversion respectively.

3.5 Deactivation

Catalysts deactivation can be an important issue in kinetic data acquisition, especially when the data acquisition is carried out for extended periods. To quantify the importance of catalysts deactivation using the HTE setup, a 300 h test was carried out with the two catalysts, loaded with different amounts to follow the deactivation at different conversion levels. Catalysts performances were measured under the same condition (220°C, 20 barg, H₂/CO = 2.12, Q_{syngas} = 2.38 NL·h⁻¹) each 4 h during the first 48 h of reaction, and each 48 h from 48 h to 300 h of reaction. Evolution of the catalyst performance with TOS is shown in Figure 6 for both catalysts, for two different catalyst loadings (200 and 350mg) operating at two conversion levels. Two periods can be distinguished: a first one showing a rapid deactivation, followed by a slower and linear deactivation starting from ~24 h of TOS. These two periods were already reported by van Berge et al.⁵¹, who associated the first one to reversible deactivation and the second one to irreversible deactivation. Todic et al.³⁹ also observed these two periods for a cobalt-alumina catalyst, respectively called initial and kinetic period. Both authors^{39,51} found a similar duration for the initial period, which is about 100 hours. A shorter period and a lower extent of deactivation are observed in our case, but deactivation phenomena are known to depend on the reactor configuration, process conditions, and catalysts^{9,14,52-54}. In particular, it has been shown that catalysts tested in milli-fixed bed reactors are less sensitive to deactivation than in conventional fixed bed reactors because of a better temperature control¹⁴. In slurry tank reactors deactivation may also be more significant than in milli-fixed bed reactors, because of catalysts attrition, and the fact that the entire catalyst bed is exposed to a high partial pressure of water. Table 4 compares

the HTE-evaluated catalyst performances at TOS 20 h to those measured in a slurry bed reactor for similar residence times and conditions (TOS 20h, 220°C, 20 barg, H₂/CO = 2.12). Both catalysts show a lower activity in the slurry bed reactor than in the milli-fixed bed reactor, with an activity 15% lower for the Co-18 catalyst and 50% lower for the Co-12 one. This difference is most likely due to the initial rapid deactivation happening in the slurry reactor, more important than in the milli-fixed bed reactor. The difference cannot be attributed to the catalyst reduction, because TPR analysis of the reduced Co-18 catalyst revealed a slightly higher DOR (74%) for the slurry experiment than the HT experiment (64%).

Figure 6 also shows that the deactivation rate depends on the CO conversion level. The catalysts working at low CO conversion levels are less deactivated during the initial period (-3.2% at 28% CO conversion against -4.4% at 42% CO conversion), and they reach the kinetic period faster than those working at high conversion. Process conditions that involve high conversion levels are indeed often associated with important deactivation⁹ because of the high generated water partial pressure⁴³, and the high carbon deposition rate⁵⁵.

Despite a limitation of the catalyst deactivation in milli-fixed bed reactors due to a better thermal control, a lower water exposure, and the absence of attrition, this phenomenon remains inevitable especially for data acquisition over extended periods of time. In case of kinetic studies, it is therefore recommended to minimize the data acquisition time since a wide range of conversion levels should be covered. It is also preferable to acquire data after the initial period of fast deactivation where the performance evolves most.

For the study of the deactivation process itself, this milli-fixed bed reactor configuration can, however, become an issue. The deactivation experiments might indeed be more time consuming than with standard slurry reactors, and should thus be preferentially carried out through accelerated aging tests in order to use efficiently the HTE technology. Such a strategy have already been used to study the long-term catalysts stability in slurry reactors¹⁵.

3.4 Contact time variations and mass transfer limitations

As discussed in section 3.2 the contact time (W/F_{CO}) is a key parameter for kinetic model development, and a frequently applied method that is used to vary this parameter, is to vary the catalyst amount between the different reactors and introduce the same flow in each reactor. We showed, however, that this strategy may lead to differences between the reactors in terms of catalyst DOR, especially for catalysts that are difficult to reduce. The other and more "conventional" method consists

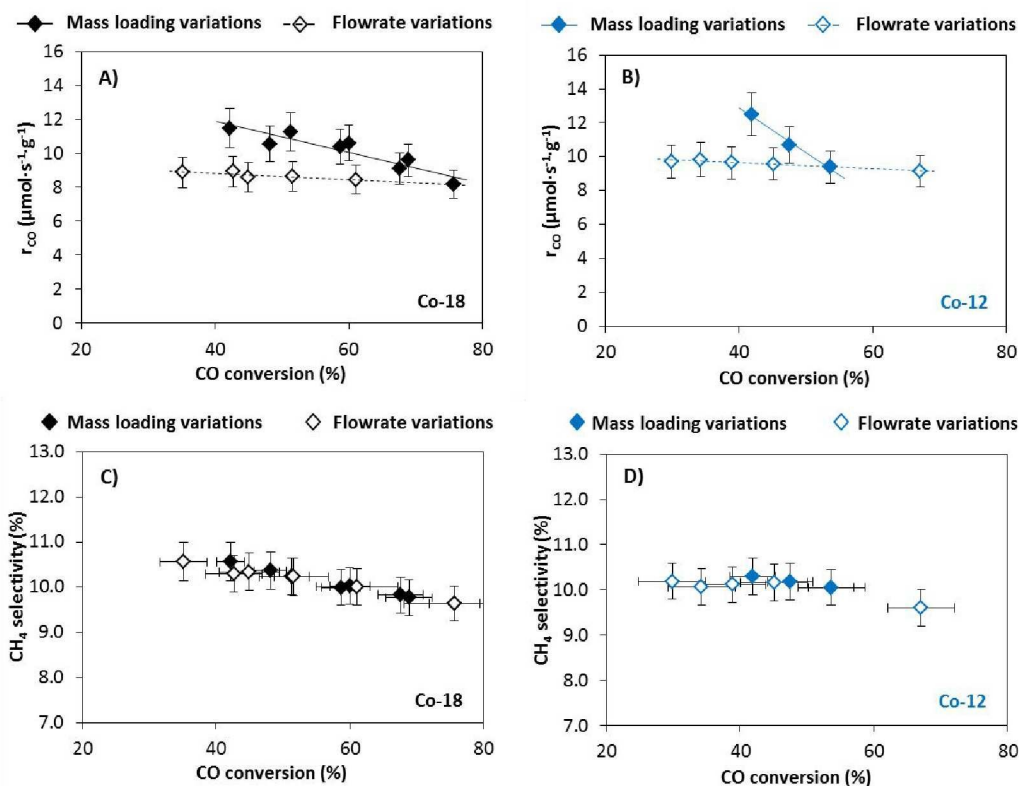


Figure 7: Impact of residence time variation method on catalysts performances measurements. Data acquired with the mass loading variation method was obtained at 220°C, 20 barg, $\text{H}_2/\text{CO} = 2.12$, 1.35 NL h^{-1} . Data acquired with the flowrate variation method was obtained at 220°C, 20 barg, $\text{H}_2/\text{CO} = 2.12$, with loadings of 453 mg and 330 mg for the Co-18 and Co-12 catalysts respectively.

of varying the syngas flowrate for a given amount of catalyst. Several issues can, however, emerge from this method: the data acquisition time increases, catalysts deactivation may interfere with the performance, and the transitory period needed to stabilize the catalyst under the new set of conditions needs to be considered.

These two methods were compared within a single test, the same test that was used to study the catalysts deactivation. In addition to the fact that different catalyst amounts were used in this test, different syngas flowrates were also applied (from 1.0 to 2.7 NL h^{-1}) during the “kinetic period”. These flowrate variations were carried out between each measurement to monitor the deactivation (performed every 48 h under the initial operating conditions). Figure 7 compares the catalyst activity measured at different CO conversion levels with the two methods, for the Co-18 catalyst (A) and the Co-12 catalyst (B) at a TOS of 24 h. Note that for the flowrate variation method the activity (r_{CO}) was corrected for the catalyst deactivation, by a factor that was estimated from the standard condition operated between each condition change. This factor corresponds more precisely to the relative CO conversion loss from the value measured at a TOS of 24 h. For the variation of the catalyst amount, performances are the one acquired at a TOS of 24 h. The two methods give a similar order of magnitude for the catalyst activity, but quite different trends are obtained regarding r_{CO} evolution with CO conversion. When flowrate variations are used, only a slight decrease of the activity with

CO conversion is measured for the two catalysts, most likely due to the CO and H_2 concentrations dependency of the kinetic law. Whereas with mass loading variations, the activity strongly decreases when the CO conversion increases (*i.e.* the mass loaded increases for a selected flow rate). This behavior is moreover more pronounced for the Co-12 catalyst than for the Co-18 one, which correlates well with its stronger DOR dependency to the hydrogen space velocity (Figure 3). The Co-12 activated at low hydrogen space velocity are less reduced, and thus less active. The activity dependency of the Co-18 catalyst cannot be explained by the DOR. The reason of its activity dependency with the amount of catalyst may rather be due to the different CO conversion levels operated during the first 24h. We have shown that the deactivation rate significantly depends on the CO conversion level, and an increase of this parameter induces an acceleration of the deactivation. Catalyst working at high conversion (large amount of catalyst) are thus more deactivated after 24h than those working at low conversion, which explains well the observed trend.

Regarding the catalyst selectivity, no major differences were observed between the two methods. A similar trend for CH_4 (illustrated on Figure 7C and D), C_{5+} , CO_2 and olefins selectivity as function of CO conversion is observed for both methods in the same proportions, and the obtained values from the two methods are comparable. This indicates that there is no effect of the reduction degree on the relationship between selectivity and CO conversion, and no deselection (*i.e.* modification of

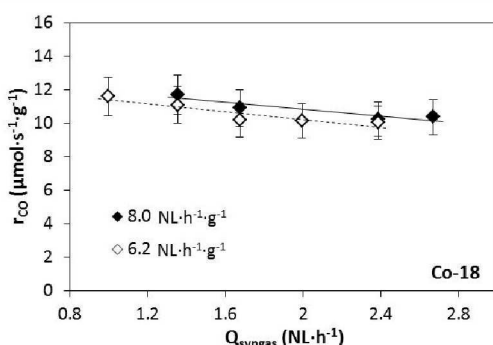


Figure 8 : Impact of gas velocity on Co-18 catalyst activity at iso-GHSV (220°C, 20 barg, $\text{H}_2/\text{CO} = 2.12$)

the selectivity with conversion correlated with TOS). It is important to note that if the catalysts were subjected to deactivation, the flowrate variation method would be inappropriate. Because of the numerous products involved in FT synthesis, a selectivity correction (as it was done for activity) would be extremely complicated to apply accurately. One should also keep in mind that when a kinetic dataset is built using the flowrate variation method, the catalysts activity correction factor has to be applied on the gas flowrate rather than the CO consumption rate in order not to modify the selectivity to conversion correlation.

The differences introduced by the hydrogen space velocity variations during catalysts reduction are therefore not only observed on the catalyst extent of reduction, but also on their performances. Besides, when different amounts of catalyst are used, they are not only activated with different gas space velocities but they are also stabilized at different conversion levels. We observed that variations of the CO conversion level during stabilisation significantly modify the catalyst performances. The mass loading method might thus not be suitable for coherent kinetic data acquisition. This observation may however depend on catalysts reducibility, susceptibility to deactivation, test duration and operating conditions. There may be some cases where catalyst reduction and stabilization are not sensitive to gas space velocity and where the first method

should be preferred, and other where catalysts are very sensitive to these parameters. This is why careful preliminary studies should be carried out on new catalysts before acquiring kinetic data, in order to use the HTE technology not only efficiently but above all in an accurate way.

The comparison of these two methods can also be used to assess the presence or absence of external mass transfer limitations, within a defined gas velocity range. Indeed, in fixed-bed reactors, external mass transfer limitations can be highlighted through gas flow velocity changes^{12,56,57}. When the reaction rate is controlled by external mass transfer instead of kinetics, an increase in linear gas velocity should increase the reaction rate. It is however important to compare performances at the same GHSV since the kinetics of the Fischer-Tropsch reaction depends on the gas composition (and thus the conversion level, proportional to the GHSV). The amount of catalyst needs thus to be adapted to compensate the gas linear velocity change in order to maintain a similar conversion level. Note that only the data obtained with the Co-18 catalyst can be used to compare performances at different gas space velocity for a selected GHSV, since the Co-12 reduction state is modified when the amount of catalyst is varied (*cf* section 3.2) in opposition to Co-18. Figure 8 shows that for a selected syngas space velocity, the increase of the gas flowrate (*i.e.* the linear gas velocity) from 1.0 to 2.7 NL h⁻¹ does not increase the activity. It can therefore be concluded that no mass transfer limitations occur within the tested range of flowrates, in full agreement with the calculated Carberry number reported in Table 1.

3.5 Pressure, temperature and syngas composition variations

In addition to the contact time (W/F_{CO}), some operating parameters influence greatly the Fischer-Tropsch kinetics such as temperature, pressure and syngas composition (H_2/CO). The effect of these parameters on the catalyst performance were studied using the HTE unit, and compared to literature. The HTE unit configuration makes it possible to run 4 reactor blocks of reactors at different temperatures. However, pressure and

Table 5 : Catalysts performances under diverse Fischer-Tropsch conditions. The data was obtained with catalysts loading of 350mg. Syngas flowrate was tuned to reach a CO conversion level of 50%.

	P (barg)	T (°C)	H ₂ /CO	GHSV (NL·h ⁻¹ ·g ⁻¹)	r_{CO} (μmol·g ⁻¹ ·s ⁻¹)	X _{CO} (%)	S _{CH4} (%)	S _{C5+} (%)	S _{CO2} (%)	O/P C ₂ -C ₅	α
Co-18	20	220	2.12	4.31	8.7	51	9.7	81.3	0.23	1.05	0.893
	20	220	1.85	3.58	7.7	49	8.7	82.6	0.26	1.24	0.899
	20	220	2.4	4.88	9.0	51	11.1	79.4	0.22	0.89	0.882
	10	220	2.12	3.58	7.7	49	8.7	82.6	0.26	1.24	0.862
	30	220	2.12	5.07	8.9	44	10.8	78.2	0.19	1.25	0.892
	20	210	2.12	2.46	4.9	50	8.6	82.4	0.19	1.32	0.907
	20	230	2.12	7.42	14.5	49	11.1	79.2	0.30	0.85	0.870
	Co-12	20	216	2.12	4.23	8.38	50	9.1	82.8	0.19	1.24
20		216	1.85	3.53	7.53	49	8.2	84.0	0.21	1.43	0.899
20		216	2.4	4.82	8.66	49	10.4	81.0	0.18	1.06	0.886
10		216	2.12	3.03	6.19	52	9.0	83.5	0.30	0.78	0.873
30		216	2.12	4.81	7.96	42	10.4	79.5	0.15	1.43	0.898
20		206	2.12	2.34	4.22	45	8.5	82.7	0.16	1.55	0.906
20		226	2.12	7.05	13.38	48	10.5	80.9	0.24	0.96	0.877

syngas composition have to be studied in a successive manner, which is not only time consuming but also detrimental to the accuracy, because of the catalyst deactivation (*cf* section 3.7). Thus, to minimize the test durations, the impact of these three parameters were studied through two separated runs. In the first one the influence of gas composition and pressure were studied, whereas in the second one, the effect of temperature and pressure were studied. Despite the possibility to perform simultaneous variations, temperature was varied successively to acquire the data on the same reactor (and thus avoid deviations due to changes of the conditions during activation or stabilisation). In practice, each of the 3 parameters studied was varied twice using a positive and a negative variation around a central value, while keeping the other parameters constant. The default values used for the Co-18 catalyst were 220°C, H₂/CO = 2.12, 20 barg while the ones used for Co-12 catalyst were 216°C, H₂/CO = 2.12, and 20 barg. The temperature was adjusted between the two catalysts to reach the same CO conversion level of 50%. The results are shown in Table 5.

It can firstly be observed that the impact of syngas composition, pressure and temperature on performances do not differ from one catalyst to the other. Thus, a general description of the observed trends is presented in the following without any distinction between catalysts. Regarding catalyst activity, CO consumption rate per gram of catalyst systematically increases when either temperature, pressure, or H₂/CO ratio increases. The positive effect of the H₂/CO increase on the activity, indicates an inhibition of the reaction by CO (*i.e.* a negative reaction order) and a promotion by H₂, which has already been reported by several authors^{58–62}. Using Arrhenius law, an apparent activation energy of 110 kJ·mol⁻¹ is obtained, which is comparable to the ones reported^{60–62}.

The parameter effect on catalyst selectivity is more complex, but in line with the trends reported in the literature^{39,61}. It can be observed that, as for the activity, the methane selectivity systematically increases when P, T or H₂/CO increases. The C₅₊ selectivity follows the opposite trend and always decreases when the CH₄ selectivity increases as observed by Lillebø et al.³⁸. However, the chain growth probability α does not obey the same correlation. When the pressure increases, the α value increases while the C₅₊ selectivity decreases, which is not expected if a perfect ASF distribution is considered. This behaviour has also been observed by Todic et al.³⁹ and may be explained by a deviation from the theoretical ASF distribution with two alpha values^{63–66}, one attributed to light products and one to heavy products. The chain growth probability of light products is negatively affected by the pressure increase while the heavy products one is positively affected. This double chain growth probability may originate from the presence of two active sites³⁹, the chain length dependency of olefins re-adsorption⁶⁷, or even products accumulation^{17,68}. The last explanation can be ruled out, since it has been verified that steady state was reached before collecting samples (*cf* next section). Concerning the CO₂ selectivity, a decrease is observed when the H₂/CO ratio increases and an increase is measured when temperature increases. CO₂ being mainly produced through the water-gas-

shift reaction in which CO is a reactant and H₂ a product, the increase of the H₂/CO ratio logically induces a CO₂ selectivity decline. Finally, the olefin-to-paraffin ratio decreases both with the increase of the H₂/CO ratio and temperature⁶⁹, but increases when the pressure increases. The increase of H₂ partial pressure has been reported to accelerate the alpha olefins secondary hydrogenation reaction³⁹ and thus a decrease of the O/P ratio. The temperature effect observed on the products selectivity might originate from differences in the activation energy of the reactions leading to the different products respectively.

The present analysis shows that general trends of activity and selectivity as a function of operating parameters corresponds well to the ones reported in the literature. It can therefore be expected that the kinetic data acquired in HTE is well representative of the one acquired in slurry reactors.

5. Conclusions

High-throughput technology is a well-suited tool for kinetic studies due to the rapid data generation capacity. In order to improve the accuracy of such equipment and make sure to acquire coherent data sets, several points require to be investigated before carrying out data acquisition. To accelerate kinetic data acquisition, it is convenient to load different amounts of the same catalyst in different reactors operated in parallel to obtain data with different contact time. However, this method may have some drawbacks and there are some cases where successive flowrate variations applied on a selected reactor might be preferred. Variation of catalyst amounts over several reactors is suitable only in the case of easily reducible catalysts, for which similar extents of reduction are obtained whatever the amount of catalyst. On the other hand, we have shown that in the case of less reducible cobalt catalysts, varying the hydrogen space velocity during activation can modify the catalyst extent of reduction and thus conduct to incoherent kinetic data. In this method, the catalysts also have to be resistant to deactivation. We observed that deactivation is directly correlated to the conversion level. The catalyst stabilization under syngas may thus differ depending on the operated conversion level and the amount of catalyst. The variation of the syngas flowrate to vary the contact time should be therefore preferred for less reducible catalysts and catalysts sensitive to deactivation. In that case, however, the catalysts need to be relatively resistant to deselection (*i.e.* loss of selectivity) to avoid incoherent data due to the evolution of performances with time on stream. When data is successively acquired, the tests duration can rapidly increase. Even with the present miniaturized HTE setup, significant transitory periods need to be considered for liquid composition analysis after a change of reaction conditions. Deactivation is thus an important phenomenon to quantify, in particular when catalysts are working at high conversion and the tests are performed for extended periods of time. This issue can still be avoided by running successive short tests. It is however time consuming and implies to consider the inter-test repeatability, which may

ARTICLE

Journal Name

be lower than the reactor-to-reactor repeatability and thus decrease the overall accuracy of a data set. The test methodology is therefore crucial to measure with accuracy the catalysts performances, and obtain a coherent data set. Moreover, different catalysts types (particles size, support, promoter) will have different reducibility and different sensitivity to deactivation, which will make it necessary to adapt the methodology for kinetic studies.

Conflicts of interest

There are no conflicts to declare.

Acknowledgements

The authors would like to thank IFP Energies nouvelles for financial and analytical support, and IRCELyon for experimental tools. Catalytic tests were conducted on the high-throughput heterogeneous catalytic platform located on Axel'One Campus facilities.

Notes and references

- S. S. Gill, A. Tsolakis, K. D. Dearn and J. Rodríguez-Fernández, *Progress in Energy and Combustion Science*, 2011, **37**, 503.
- D. Farrusseng, *Surface Science Reports*, 2008, **63**, 487.
- P. Boldrin, J. R. Gallagher, G. B. Combes, D. I. Enache, D. James, P. R. Ellis, G. Kelly, J. B. Claridge and M. J. Rosseinsky, *Chemical science*, 2015, **6**, 935.
- P. Munnik, N. A. Krans, P. E. de Jongh and K. P. de Jong, *ACS Catal.*, 2014, **4**, 3219.
- G. F. Botes, T. C. Bromfield, R. L.J. Coetzer, R. Crous, P. Gibson and A. C. Ferreira, *Catalysis and synthetic fuels: state of the art and outlook*, 2016, **275**, 40.
- S. Sartipi, H. Jansma, D. Bosma, B. Boshuizen, M. Makkee, J. Gascon and F. Kapteijn, *Review of Scientific Instruments*, 2013, **84**, 124101.
- X. Hua, L. Wang, Y. Xu, Y. Wang and Z. Gao, *CHINESE JOURNAL OF CATALYSIS (CHINESE VERSION)*, 2014, **32**, 1242.
- J. H. den Otter, S. R. Nijveld and K. P. de Jong, *ACS Catal.*, 2016, **6**, 1616.
- T. O. Eschemann and K. P. de Jong, *ACS Catal.*, 2015, **5**, 3181.
- J. K. van der Waal, G. Klaus, M. Smit and C. M. Lok, *Catalysis and synthetic fuels: state of the art and outlook*, 2011, **171**, 207.
- C. Cao, D. R. Palo, A. L. Y. Tonkovich and Y. Wang, *Catalysis and synthetic fuels: state of the art and outlook*, 2007, **125**, 29.
- J.A. Moulijn, J. Pérez-Ramírez, R.J. Berger, G. Hamminga, G. Mul and F. Kapteijn, *Catalysis Today*, 2003, **81**, 457.
- J. Pérez-Ramírez, R. J. Berger, G. Mul, F. Kapteijn and J. A. Moulijn, *Catalysis Today*, 2000, **60**, 93.
- S. Chambrey, P. Fongarland, H. Karaca, S. Piché, A. Griboval-Constant, D. Schweich, F. Luck, S. Savin and A.Y. Khodakov, *Catalysis Today*, 2011, **171**, 201.
- C. Boyer, J. Gazarian, V. Lecocq, S. Maury, A. Forret, J. M. Schweitzer and V. Souchon, *Oil Gas Sci. Technol. – Rev. IFP Energies nouvelles*, 2016, **71**, 44.
- Dry Mark E. in *Handbook of Heterogeneous Catalysis*, American Cancer Society, 2008.
- K. Xiao, X. Qi, X. Wang, D. Lv, M. Zhu and L. Zhong, *Catal Lett*, 2017, **147**, 704.
- G. Morra, D. Farrusseng, E. Guillon, S. Morin, C. Bouchy, P. Duchêne and C. Mirodatos, *Catalysis Today*, 2008, **137**, 71.
- D. Nabaho, J. W. Niemantsverdriet, M. Claeys and E. van Steen, *Recent Advances in F-T Synthesis and Fuel Processing Catalysis*, 2016, **261**, 17.
- H. Bartholomew, *Catalysis Letters*, 1990, **7**, 27.
- W. L. Roth, *Journal of Physics and Chemistry of Solids*, 1964, **25**, 1.
- M. Claeys, M. E. Dry, E. van Steen, E. Du Plessis, P. J. van Berge, A. M. Saib and D. J. Moodley, *Journal of Catalysis*, 2014, **318**, 193.
- L. J. E. Hofer, E. M. Cohn and W. C. Peebles, *J. Phys. Chem.*, 1949, **53**, 661.
- P. Cossee, *Journal of Inorganic and Nuclear Chemistry*, 1958, **8**, 483.
- Peter Mohn, *Magnetism in the Solid State An Introduction*, Springer Science & Business Media, 2006.
- EUROKIN spreadsheet on requirements for measurement of intrinsic kinetics in the gas-solid fixed-bed reactor. https://eurokin.org/wp-content/uploads/downloads/2019/08/EUROKIN_fixed-bed_html_guide.pdf.
- R. B. Anderson, R. A. Friedel and H. H. Storch, *The Journal of Chemical Physics*, 1951, **19**, 313.
- P. G. Dimitrova and D. R. Mehandjiev, *Journal of Catalysis*, 1994, **145**, 356.
- P. Arnoldy and J. A. Moulijn, *Journal of Catalysis*, 1985, **93**, 38.
- A. Y. Khodakov, W. Chu and P. Fongarland, *Chemical reviews*, 2007, **107**, 1692.
- B. Ernst, A. Bensaddik, L. Hilaire, P. Chaumette and A. Kiennemann, *Catalysis Today*, 1998, **39**, 329.
- P. A. Chernavskii, G. V. Pankina, A. S. Lermontov and V. V. Lunin, *Kinetics and Catalysis*, 2003, **44**, 657.
- N. E. Tsakoumis, R. E. Johnsen, W. van Beek, M. Rønning, E. Rytter and A. Holmen, *Chemical communications (Cambridge, England)*, 2016, **52**, 3239.
- C. H. Bartholomew, *Journal of Catalysis*, 1976, **45**, 41.
- Yulong Zhang, Dongguang Wei, Sonia Hammache and James G. Goodwin, *Journal of Catalysis*, 1999, **188**, 281.
- J. Paterson, M. Peacock, E. Ferguson, M. Ojeda and J. Clarkson, *Applied Catalysis A: General*, 2017, **546**, 103.
- G. L. Bezemer, J. H. Bitter, Kuipers, Herman P. C. E., H. Oosterbeek, J. E. Holeywijn, X. Xu, F. Kapteijn, A. J. van Dillen and K. P. de Jong, *J. Am. Chem. Soc.*, 2006, **128**, 3956.

38. A. Lillebø, E. Rytter, E. A. Blekkan and A. Holmen, *Ind. Eng. Chem. Res.*, 2017, **56**, 13281.
39. Branislav Todić, Wenping Ma, Gary Jacobs, Burtron H. Davis and Dragomir B. Bukur, *Journal of Catalysis*, 2014, **311**, 325.
40. E. Iglesia, *Applied Catalysis A: General*, 1997, **161**, 59.
41. D. B. Bukur, Z. Pan, W. Ma, G. Jacobs and B. H. Davis, *Catal Lett*, 2012, **142**, 1382.
42. A.-M. Hilmen, O. A. Lindvåg, E. Bergene, D. Schanke, S. Eri and A. Holmen in *Studies in Surface Science and Catalysis Natural Gas Conversion VI*, ed. E. Iglesia, J.J. Spivey and T.H. Fleisch, Elsevier, 2001, p 295.
43. Jinlin Li, Xiaodong Zhan, Yongqing Zhang, Gary Jacobs, Tapan Das and Burtron H Davis, *Applied Catalysis A: General*, 2002, **228**, 203.
44. S. Storsæter, Ø. Borg, E. A. Blekkan and A. Holmen, *Journal of Catalysis*, 2005, **231**, 405.
45. M.-C. Marion and F. Hugues in *Studies in Surface Science and Catalysis Natural Gas Conversion VIII*, ed. F. Bellot Noronha, M. Schmal and E. Falabella Sousa-Aguiar, Elsevier, 2007, p 91.
46. I. C. Yates and C. N. Satterfield, *Energy Fuels*, 1992, **6**, 308.
47. W. Ma, G. Jacobs, Y. Ji, T. Bhatelia, D. B. Bukur, S. Khalid and B. H. Davis, *Top Catal*, 2011, **54**, 757.
48. H. Schulz, Z. Nie and F. Ousmanov, *Fischer-Tropsch synthesis on the eve of the XXI Century*, 2002, **71**, 351.
49. B. Shi and B. H. Davis, *Applied Catalysis A: General*, 2004, **277**, 61.
50. A. M. Saib, D. J. Moodley, I. M. Ciobîcă, M. M. Hauman, B. H. Sigwebela, C. J. Weststrate, J. W. Niemantsverdriet and J. van de Loosdrecht, *Catalysis Today*, 2010, **154**, 271.
51. P. J. van Berge and R. C. Everson in *Studies in Surface Science and Catalysis Natural Gas Conversion IV*, ed. M. de Pontes, R.L. Espinoza, C.P. Nicolaidis, J.H. Scholtz and M.S. Scurrall, Elsevier, 1997, p 207.
52. M. Sadeqzadeh, S. Chambrey, J. Hong, P. Fongarland, F. Luck, D. Curulla-Ferré, D. Schweich, J. Bousquet and A. Y. Khodakov, *Ind. Eng. Chem. Res.*, 2014, **53**, 6913.
53. N. E. Tsakoumis, M. Rønning, Ø. Borg, E. Rytter and A. Holmen, *Catalysis Today*, 2010, **154**, 162.
54. J. Clarkson, P. R. Ellis, R. Humble, G. J. Kelly, M. McKenna and J. West, *Applied Catalysis A: General*, 2018, **550**, 28.
55. D. Peña, A. Griboval-Constant, V. Lecocq, F. Diehl and A. Y. Khodakov, *Catalysis Today*, 2013, **215**, 43.
56. J. H. Yang, H.-J. Kim, D. H. Chun, H.-T. Lee, J.-C. Hong, H. Jung and J.-I. Yang, *Fuel Processing Technology*, 2010, **91**, 285.
57. St. Walter, St. Malmberg, B. Schmidt and M. A. Liauw, *Catalysis Today*, 2005, **110**, 15.
58. R. A. van Santen, A. J. Markvoort, I. A. W. Filot, M. M. Ghouri and E. J. M. Hensen, *Physical chemistry chemical physics PCCP*, 2013, **15**, 17038.
59. P. K. Agrawal, J. R. Katzer and W. H. Manogue, *Journal of Catalysis*, 1981, **69**, 312.
60. K. Keyvanloo, S. J. Lanham and W. C. Hecker, *Catalysis Today*, 2016, **270**, 9.
61. R. Zennaro, Tagliabue M. and C. H. Bartholomew, *Catalysis Today*, 2000, **58**, 309.
62. W. Chen, I. A. W. Filot, R. Pestman and E. J. M. Hensen, *ACS catalysis*, 2017, **7**, 8061.
63. J. Patzlaff, Y. Liu, C. Graffmann and J. Gaube, *Applied Catalysis A: General*, 1999, **186**, 109.
64. T. J. Donnelly, I. C. Yates and C. N. Satterfield, *Energy Fuels*, 1988, **2**, 734.
65. T. J. Donnelly and C. N. Satterfield, *Applied Catalysis*, 1989, **52**, 93.
66. R. A. Dictor and A. T. Bell, *Journal of Catalysis*, 1986, **97**, 121.
67. E. W. Kuipers, I. H. Vinkenburg and H. Oosterbeek, *Journal of Catalysis*, 1995, **152**, 137.
68. B. Shi and B. H. Davis, *Applied Catalysis A: General*, 2004, **277**, 61.
69. Y. Dai, F. Yu, Z. Li, Y. An, T. Lin, Y. Yang, L. Zhong, H. Wang and Y. Sun, *Chin. J. Chem.*, 2017, **35**, 918.

